Acta Pharmaceutica Sinica B 2013;3(6):400–407

Institute of Materia Medica, Chinese Academy of Medical Sciences
Chinese Pharmaceutical Association

Acta Pharmaceutica Sinica B

www.elsevier.com/locate/apsb
www.sciencedirect.com

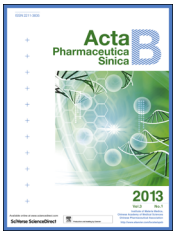

ORIGINAL ARTICLE

Characterization of a dextran–coated layered double hydroxide acetylsalicylic acid delivery system and its pharmacokinetics in rabbit

Li-e Dong, Guojing Gou*, Lin Jiao

Medical Chemistry Department, School of Basic Medicine, Ningxia Medical University, Yinchuan 750004, China

Received 24 July 2013; revised 20 August 2013; accepted 23 September 2013

KEY WORDS

Controlled release;
Acetylsalicylic acid;
Dextran;
Layered double hydroxide;
Pharmacokinetics;
Rabbit

Abstract The aim of this study was to prepare a dextran–coated layered double hydroxide acetylsalicylic acid (DEX–LDH–ASA) delivery system by co-precipitation of LDH–ASA and its *in-situ* compositing with DEX. The structure of the system was investigated using X-ray diffraction (XRD), Fourier transform infrared spectroscopy (FT-IR) and thermogravimetry (TG). Its *in vitro* drug release properties and *in vivo* pharmacokinetics in rabbit were also determined. The results show that the DEX–LDH–ASA system retained the crystal structure of LDH–ASA and gave a marked improvement in its dispersion. It also prolonged the release of ASA and shifted the release pattern from first-order to zero-order kinetics. The pharmacokinetics of ASA administered in the DEX–LDH–ASA system to rabbits produced two absorption peaks with a C_{max} of 14.8 ± 1.7 mg/L at 2.11 ± 0.69 h and an elimination half-life of 2.25 ± 0.84 h for the first peak. The fact that delivery of ASA in the DEX–LDH–ASA system was sustained with improved bioavailability indicates the potential of the system as a controlled release formulation with application to other drugs.

*Corresponding author. Tel.: +86 13895652708.
E-mail address: ggj1964@163.com (Guojing Gou).

Peer review under responsibility of Institute of Materia Medica, Chinese Academy of Medical Sciences and Chinese Pharmaceutical Association.

Production and hosting by Elsevier

2211-3835
http://dx.doi.org/10.1016/j.apsb.2013.09.003

1. Introduction

Traditionally acetylsalicylic acid (ASA) has been used as an antipyretic, analgesic and antiinflammatory drug marketed under the trade name aspirin. Extensive clinical research has shown that ASA is useful in the prevention of cerebral thrombosis, coronary heart disease, myocardial infarction, ischemic stroke, transient ischemic attack, unstable angina and postoperative thrombosis. However, oral administration of ASA is associated with severe irritation to the gastrointestinal tract mucosa leading to a number of adverse effects including nausea, vomiting, ulceration and bleeding. To reduce these adverse effects and maintain or even improve its beneficial effects has led to the development of some oral controlled release systems[1–4].

Layered double hydroxide (LDH), also known as hydrotalcite-like material or anionic clay, is a supramolecular material consisting of layers of electropositive hydroxides of divalent (M^{II}) and trivalent (M^{III}) metals and interlayer anions (A^{m-})[5]. LDH is currently described by the general formula $[M^{II}_{1-x}M^{III}_{x}(OH)_2]^{x+}(A^{m-})_{x/m}\cdot nH_2O$, where x represents the ratio of $[M^{3+}]/([M^{2+}]+[M^{3+}])$. Due to the anion exchange properties of LDH, many pharmaceutically active compounds have been intercalated into the interlayer of LDH including anticancer, antiinflammatory, antihypertensive and cardiovascular drugs [6–15]. Owing to electrostatic interactions and solid geometry, intercalated drugs are stabilized and usually released in a sustained manner[6–12]. Early research demonstrated that intercalation of antiinflammatory drugs in the LDH–drug delivery system changed their release profile[7,8], improved their solubility and reduced their adverse effects[9]. However, due to the alkalinity of the LDH laminate, the use of orally administered LDH–drug delivery systems still remains somewhat problematic[8].

Dextran (DEX), an α-D-pyran polysaccharide, is a relatively non-toxic, biodegradable and water-soluble macromolecule[16] commonly used as an auxiliary material for colonic targeting of drugs[17]. Its large network of hydroxyl and 1,6-α-glycosidic bonds makes it suitable to provide a protective layer over the LDH–drug system to eliminate the acid corrosion for the LDH laminate[18–20]. Taking advantage of this, we assembled a supramolecular ASA delivery system composed of LDH loaded ASA with a DEX coating on the surface. The present study was undertaken to elucidate the structure of this DEX–LDH–ASA system and evaluate its *in vitro* ASA release profile and ASA pharmacokinetics after oral administration in rabbit.

2. Materials and methods

2.1. Materials

ASA (BR) was purchased from the Fourth Pharmaceutical Co. Ltd. (Zhonglian Group, Wuhan, China). Magnesium chloride ($MgCl_2\cdot 6H_2O$), aluminum chloride ($AlCl_3\cdot 6H_2O$) and potassium dihydrogen phosphate ($KH_2PO_4\cdot H_2O$) were analytical grade from Laiyang Chemical Co., Ltd. (Shandong, China). Salicylic acid (SA) was analytical grade from the China Institute of Food and Drug Control. Benzoic acid and ethyl acetate were purchased from the North Sky Medicinal Chemistry Reagent Factory (Tianjin, China). HPLC grade methanol was purchased from Jiangtian Chemical Technology Co., Ltd. (Tianjin, China). Deionized water was used in all experiments. Healthy rabbits ($n=12$, weight 2.5 ± 0.3 kg) were supplied by the Animal Center of Ningxia Medical University.

2.2. Instrumentation

Powder X-ray diffraction (XRD) patterns were recorded in the range 5–80° on a Rigaku D/Max-rB diffractometer using Cu K_α radiation ($\lambda=0.1542$ nm) at 30 kV and 30 mA and a dwell time of 2° per minute. Fourier transform infrared spectra (FT-IR) were recorded in the range 400–4000 cm^{-1} on a TENEOR27 IR spectrophotometer (Brooke Company, Germany) with 4 cm^{-1} resolution using the KBr disc method. Particle size was determined using a United States PSS NICOMPTM 380 submicron particle size analyzer. Analysis of ASA to determine its loading and release rate was carried out using a Unico UV-3802 UV/VIS spectrophotometer (Unico Instrument Co. Ltd., Shanghai, China). Blood concentrations of SA were determined by HPLC on a HITACHI 2000 HPLC system equipped with an Allsphere ODS column (250 mm × 4.6 mm, 5 μm) maintained at 25 °C using a mobile phase of methanol:pH 6.8 KH_2PO_4 buffer (1:3, *v/v*) at a flow rate of 1 mL/min. Detection was by UV absorption at 240 nm.

2.3. Synthesis of the DEX–LDH–ASA system

The intercalated LDH–ASA complex was prepared using the co-precipitation method[8,13,18]. An aqueous 2.0 M NaOH solution was added dropwise to 850 mL of an aqueous, magnetically stirred (300 rpm) solution containing $MgCl_2\cdot 6H_2O$ (40.82 g), $AlCl_3\cdot 6H_2O$ (24.30 g) and ASA (72.83 g) maintained at 80 °C under a nitrogen atmosphere. When the pH reached 10.6, the slurry was maintained at 80 °C for a further 30 min to produce the aged slurry. To obtain the solid LDH–ASA complex, the slurry was centrifuged and the solid material collected, washed sequentially with water, ethanol and diethyl ether and finally dried in an oven at 65 °C. The solid product was denoted L_2 (LDH–ASA secondary compound).

An aqueous solution containing 32.20 g dextran in 200 mL deionized water was added to the aged magnetically stirred LDH–ASA slurry prepared as described above. The hot slurry was then poured into 100 mL cold ethanol which was previously maintained at −80 °C for 24 h to segregate solid with the method of *in situ* solvent conversion[18,19]. The ethanol suspension was maintained under a nitrogen atmosphere for 3 h at room temperature before being centrifuged, washed with water and finally dried in an oven at 60 °C. The product was denoted L_3 (DEX–LDH–ASA triple composite).

2.4. In vitro release of ASA from the LDH–ASA system

2.4.1. Drug loading

The L_2 and L_3 samples were powdered in a pestle and mortar and sifted through a 100-mesh screen. Samples (0.2000 g) of powders were then dissolved in the minimum amount of concentrated HCl, transferred to 50 mL volumetric flasks and made up to volume. An aliquot (5 mL) was removed, filtered through a 0.22 μm filter membrane and 2.00 mL of the filtrate diluted to 10.00 mL. The ASA concentration in this solution was then determined from its absorption at 303 nm. All experiments were carried out in triplicate. The results showed that the drug loadings of ASA in L_2 and L_3 were 28.2% and 13.5%, respectively.

2.4.2. Drug release of ASA

Drug release profiles were determined in phosphate buffered saline (PBS, pH 7.50) at 37 ± 0.5 °C using a closed circulation system.

Before measurement, the system was cleaned by pumping doubly-distilled water until the absorbance of the ultraviolet detector remained at zero. After draining the system by operating the pump in the opposite direction for 15 min, 500 mL PBS solution was introduced through a 0.22 μm filter and circulated in the forward direction while the detector was adjusted to zero. A sample (0.2500 mg) of L_2 or L_3 was then added to the dissolution cup and the absorbance and pH monitored for 60 min using a rotation speed of 100 rpm.

2.5. *Pharmacokinetic study in rabbit*

2.5.1. *Animal protocol*

The single-dose, open-label, randomized, two-period crossover study was approved by the Ethics Committee for Animal Experimentation of Ningxia Medical University. Animals were fasted with *ad libitum* access to water for 12 h before dosing to 4 h after dosing. Rabbits were administered by gavage an aqueous suspension of 50 mg ASA by gavage as either DEX–LDH–ASA or pure ASA with a 1-week washout period. Blood samples (2.5 mL) were collected from the auricular vein into heparinized tubes before drug administration and after pure aspirin at 0.25, 0.40, 0.60, 0.80, 1.0, 1.25, 1.40, 1.70, 2.0, 2.25, 2.50, 3.0 and 4.0 h and after DEX–LDH–ASA at 0.11, 0.19, 0.5, 1, 2, 4, 6, 8, 10, 12, 14, 16, 18, 23.5, 28, 33, 37, 41, 55 and 60.5 h. Blood samples were centrifuged immediately at 3000 rpm for 15 min and plasma stored at −20 °C in coded glass tubes pending analysis.

2.5.2. *HPLC assay*

Plasma concentrations of SA were determined by HPLC using benzoic acid as internal standard (IS) because ASA was ultimately translated into SA *in vivo*. Stock solutions of SA and benzoic acid (1 mg/mL) were prepared in methanol and diluted to obtain an 0.1 mg/mL SA standard solution and an 0.1 mg/mL working IS solution respectively. Aliquots (500 μL) of blank rabbit plasma were then spiked with SA standard solution to give calibration standards with concentrations of 0.1, 0.5, 1, 2, 4, 10, 16, 24 and 32 mg/mL[1,4]. Quality control (QC) samples (1, 10 and 60 mg/mL) were prepared in the same way.

Plasma samples were thawed at room temperature and 500 μL aliquots pipetted into Eppendorf tubes. After adding 20 μL aliquots of IS working solution, the mixture was vortex mixed and 200 μL aliquots of monopotassium phosphate buffer (0.5 M filtered through 0.45 μm filters) added. After shaking for 1–2 min, 3 mL ethyl acetate was added and the samples vortexed for 10 min and centrifuged for 15 min at 3000 rpm. Upper organic layers were transferred to clean tubes and the aqueous phase extracted again with 2 mL ethyl acetate. The two extracts were mixed and evaporated to dryness in a vacuum drying oven at 0.8 mPa and 55 °C. Residues were reconstituted in 300 μL monopotassium phosphate solution (0.025 M), vortexed for 10 min and centrifuged at 3000 rpm for 15 min. Finally samples were filtered through 0.22 μm filters and 20 μL aliquots injected into the HPLC system. Concentration of SA was determined from peak areas of analyte and IS.

The assay was linear ($C = 1.2704 + 3.1662\ R$, $r^2 = 0.9942$) with a limit of quantitation of 0.1 mg/L. Results of assay validation for recovery and precision based on QC samples are shown in Table 1. The results show the method was satisfactory for the determination of SA in biological samples[1–4].

2.5.3. *Pharmacokinetic analysis*

Pharmacokinetic parameters were determined from plasma concentration–time curves using the DAS 2.0 method. The maximum observed concentration (C_{max}) and time to C_{max} (T_{max}) were read directly from the data. Areas under plasma concentration–time curves (AUCs) were calculated using the linear trapezoidal rule from time zero to t (AUC_{0-t}).

3. Results and discussion

3.1. *Characterization of the ASA-loaded LDH delivery system*

The X-ray diffraction patterns of L_2 and L_3 are depicted in Fig. 1. Fig. 1A represents the XRD of $Mg_6Al_2(OH)_{12} \cdot 4.5H_2O$ recorded by the standard card 35-0965 of the Joint Committee on Powder Diffraction Standards which represents the standard model of the R-3m [166] crystal system. Fig. 1B shows the 003, 006, 0012, 0015, 0018, 110 and 113 reflections of sample L_2 were found for 2θ at 11.220°, 22.501°, 34.476°, 38.648°, 45.588°, 60.560° and 61.794°, respectively. The basal spacing scope and the intensity distribution characteristics of L_2 were generally consistent with those of the 35-0965 model suggesting that the crystal form of LDH is maintained in the LDH–ASA intercalated system. The basal spacing of d_{110} (0.1528 nm) and d_{113} (0.1500 nm) were close to those of the 35-0965 standard but the d_{003}, d_{006}, d_{012}, d_{015} and d_{018} values of L_2 were greater than those of the standard indicating that the OH^- and Cl^- ions in the interlayer of LDH have been replaced by ASA[13]. The reflection line of the d_{110} diffraction peak in the LDH–ASA system was unchanged in the intercalation process indicating that the intercalation of ASA did not change the structure of the laminate[6,9,12]. Fig. 1C shows the diffraction parameters of 003, 006, 0012, 0015, 0018, 110 and 113 in the L_3 sample were (11.279°, 0.7839 nm), (22.439°, 0.3959 nm), (34.259°, 0.2615 nm), (38.125°, 0.2359 nm), (44.799°, 0.2021 nm), (60.597°, 0.1527 nm) and (61.961°, 0.1496 nm), respectively. The diffraction variations in L_3 were similar to those in L_2 compared with the 35-0965 standard as confirmed by the shifting of the 006, 0012, and 0015 diffraction peaks to low 2θ angles at 22.439°, 34.259° and 38.125°,

Table 1 Results of the determination of recovery and precision for the HPLC assay of salicylic acid in rabbit plasma ($n = 5$).

Spiked concentration (μg/mL)	Concentration found (μg/mL)	Recovery (%)	Precision (RSD %)	
			Intra-day	Inter-day
1.0	0.852 ± 0.025	85.2 ± 2.5	3.56 ± 0.11	8.91 ± 0.21
10	9.76 ± 0.28	97.6 ± 2.8	2.70 ± 0.08	6.65 ± 0.13
16	16.54 ± 0.50	103.4 ± 3.1	2.84 ± 0.08	4.06 ± 0.04

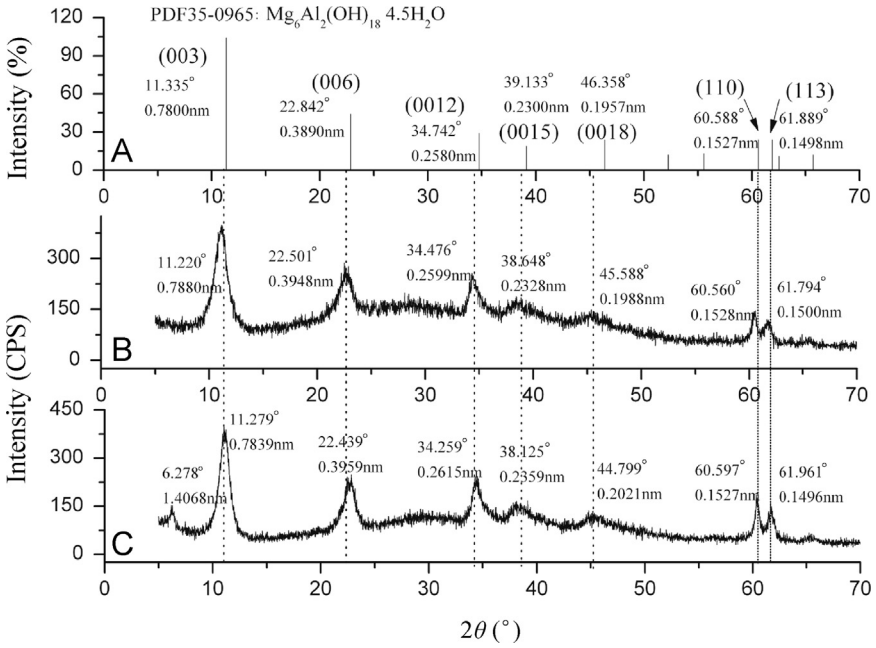

Figure 1 XRD patterns of (B) L_2 and (C) L_3.

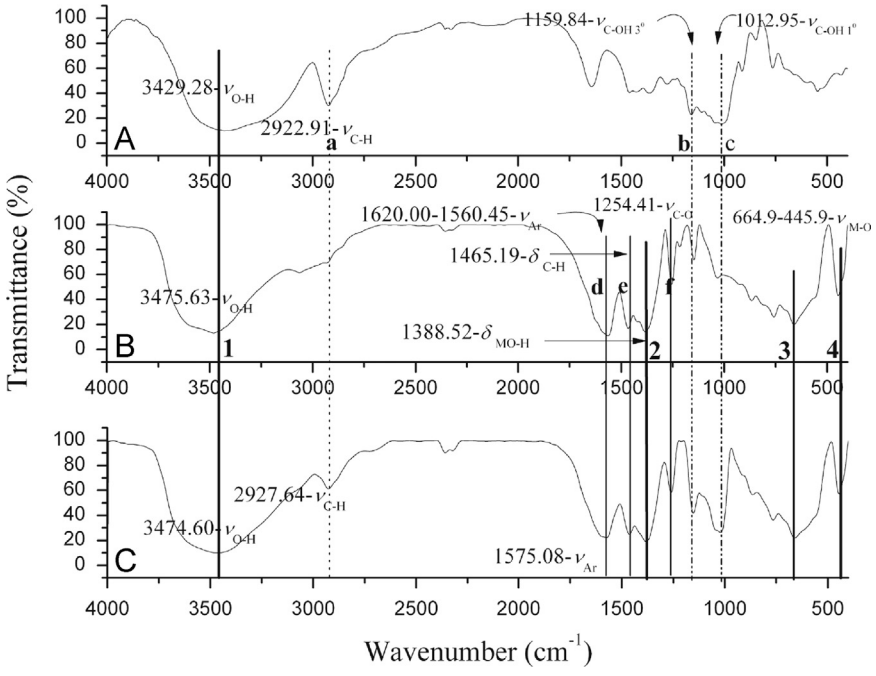

Figure 2 IR spectra of (A) DEX, (B) L_2 and (C) L_3.

respectively with d_{110} values equal to those in the 35-0965 standard. A new peak was found at 6.278° (Fig. 1C, $d = 1.4068$ nm) and assigned to the diffraction location of the amorphous organic polymer. This indicates that the organic phase of DEX was actually deposited on the surface of L_2 rather than intercalated into its interlayer spaces. Overall, the results of XRD analysis show that combination with DEX did not change the crystal structure of the LDH–ASA intercalation system. However, modifying the LDH–drug delivery system with organic composites will weaken the ionization of the LDH crystal plane, reduce the toxicity of the loaded drug to biological tissue and improve the cell targeting efficiency of the LDH delivery system[17].

The FT-IR spectra of DEX, L_2 and L_3 are compared in Fig. 2. DEX showed an intense broad band at 3429.28 cm^{-1} which can be assigned to the O–H stretch and the sharp absorption peak (marked with a in Fig. 2A) at 2922.91 cm^{-1} can be assigned to a C–H vibration. The band at 1159.84 cm^{-1} (marked with b) is due to ν^{C-OH} in DEX and the band at 1012.95 cm^{-1} is due to ν^{C-OH} in $-CH_2-OH$. The FTIR spectra of L_2 showed many intense, sharp absorption peaks, reflecting the different functional groups present

in the supramolecular composite. The broad absorption peak at 3475.63 cm^{-1} mainly arises from the O–H stretch in LDH present within the hydrate layer[6,9,12,13]. The absorption peak 2 at 1388.52 cm^{-1} is due to the out-of-plane rocking vibration of an H atom outside the LDH laminate[13], while peaks 3 at 664.9 cm^{-1} and 4 at 445.9 cm^{-1} are assigned to metal–oxygen stretches within the LDH layer[6,9,12]. These typical bands (marked by 1–4) correspond to ν^{O-H}, δ^{MO-H} and ν^{M-O-M} stretches indicating that the structure of LDH is maintained during the intercalation process[12,13,18]. The spectrum of L_2 in Fig. 2B also shows the specific bands of ASA (marked with d, e and f) demonstrating that ASA anions are intercalated into the interlayer galleries of LDH. In detail, the intense, broad absorption band at 1620.0–1560.45 cm^{-1} is attributed to the ring vibration mode ν_{Ar} while the peaks at 1465.19 and 1254.41 cm^{-1} are assigned to the δ_{C-H} deformation mode and ν_{C-O} stretch respectively of ester bonds in ASA. The FTIR spectrum of L_3 shown in Fig. 2C clearly includes the main absorption peaks of DEX, ASA and LDH. The absorption bands assigned to L_2 are found at 3474.60, 1386.49, 666.84 and 447.12 cm^{-1} and attributed to the ν_{O-H}, δ_{MO-H} and ν_{M-O} stretches of LDH, respectively. The increased absorption area and wavelength range at 3474.60 cm^{-1} for L_3 presumably occurs due to a three-way merger of the ν^{O-H} mode present in LDH, DEX and ASA[18]. In addition, the absorption peaks of intercalated ASA corresponding to ν_{Ar}, δ_{C-H} and ν^{C-O} of ASA (d, e, and f, respectively) of L_2 are found in Fig. 2C at 1575.08, 1460.35, and 1258.81 cm^{-1} respectively. The characteristic vibrations of DEX, including ν^{C-H} and ν^{C-OH} (corresponding to a, b and c) appear at similar locations in Fig. 2C. The spectrum of L_3 shows the specific bands of intercalated ASA, supporting LDH and surface composite DEX but does not appear as a simple superposition of these components indicating L_3 is a supramolecular assembly rather than a simple mixture of DEX, LDH and ASA.

The thermal behavior of L_2 and L_3 nanoparticles was examined using thermogravimetric (TG) and differential thermogravimetric (DTG) analyses. The results are shown in Fig. 3. Two main thermal events are clearly observed in L_2 (Fig. 3A). The first occurs in the region 68.5–158.2 °C and is attributed to the removal of adsorbed water on the external surface of LDH and water within the interlayer of L_2[12,13]. This corresponds to a sharp peak in the differential thermogravimetric curve at 115.6 °C with 5.551% weight loss and an enthalpy 46.58 J/g. The second event occurs in the region 272.8–434.9 °C and can be attributed to dehydroxylation of the metal hydroxide layers and decomposition and subtle combustion of intercalated ASA. This corresponds to the strong endothermic peak at 345.9 °C with 18.61% weight loss and an enthalpy of 801.1 J/g. The final stage of weight loss is related to the formation of spinel LDO[9,16]. Fig. 3B shows that L_3 exhibits more complicated thermal behavior than L_2 and takes place in three major stages of weight loss. These occurred at temperature maxima of 112 °C, 290.3 °C and 425.2 °C with weight losses of 6.476%, 20.02% and 12.32%, respectively, The first stage of weight loss in the range 66.1–168.7 °C can be attributed to the removal of adsorbed and structured water; it displays a temperature interval similar to that seen in L_2 but with an enthalpy value up to 2.75 times higher. This suggests that the elimination of adsorbed water is more difficult in the three-level composite and that the removal of interlaminar water from LDH is also more limited. Compared with L_2, the mass loss increased by 0.925% in the same temperature range which can be attributed to the partial evaporation of DEX. The second stage of weight loss occurred in the region 209.6–311.4 °C corresponding to a small endothermic section in the DSC curve at 243.3 °C with 9.735% weight loss and an enthalpy of 53.3 J/g. This was followed by another event in the range 331.4–420.1 °C corresponding to a strong broad peak at 373.2 °C with 10.28% weight loss and an enthalpy of 271.4 J/g. The total weight loss of the two successive events (20.02%) was greater than that of L_2 (18.61%) in the region 272.8–434.9 °C but the total enthalpy value (324.7 J/g) was about 40% of L_2. The variation in slopes of the DSC and DTG curves shows that the dehydroxylation of the metal hydroxide layers and the decomposition of the intercalated ASA is divided into at least two sections which usually overlap during the second stages of weight loss in the LDH–ASA system[9,16]. It has been suggested that the intercalated material may be involved in the dehydroxylation process of LDH to form spinel LDO *via* grafting with LDH and replacing hydroxyl groups to promote dehydration, condensation and phase transformation of the hydroxide laminate[5,13]. In the three-level composite, the endothermic enthalpy of decomposition of the LDH laminate decreases and the event is clearly separated from the subsequent thermal decomposition. This demonstrates that ASA intercalated between interlayers of the LDH and the

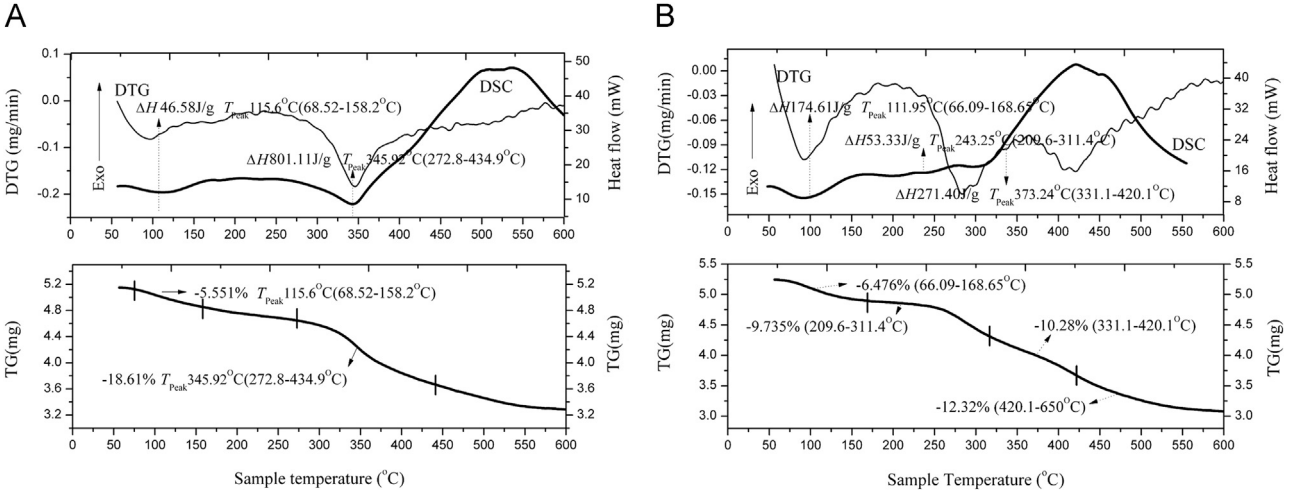

Figure 3 Thermal analysis curves of (A) L_2 and (B) L_3.

DEX coating outside LDH may both be involved in the dehydroxylation process leading to the dramatic decline in activation energy. The disintegration of the residual solid was also facilitated by the organic functional groups inside and outside the LDH laminate.

The results of particle size determination showed that for L_2 the mean particle diameter was 184.2 nm with a distribution range of 20–354 nm and for L_3 was 54.9 nm with a distribution of 15–68.3 nm. The smaller size and narrower distribution range of L_3 indicates that the dispersion of the ASA-loaded particle is improved by DEX. This is most likely due to the inhibition by DEX of aggregation of the nanoparticles during the drying process[18].

3.2. *In vitro release of ASA from the LDH–ASA system*

The cumulative release profiles of L_2 and L_3 in PBS (pH 7.50) are compared in Fig. 4. Release of ASA from L_2 was very rapid with a clear burst effect occurring over 0–4 min and releasing 73.3% of the drug. This is probably due to the reduced barrier to release of drug adsorbed outside the LDH laminate in powder state. This quick release was followed by a slower release over 56 min which occurs by exchange of ASA ions and phosphate ions in the buffer as previously reported[8,12,14,15]. The reduced barrier to drug release also results in a slight burst effect for L_3 but, in this case, only 30% ASA was released over 0–4 min indicating that the majority of drug is encapsulated inside the DEX–LDH–ASA nanocomposite. The release profile of L_3 shows that 45% of the drug was released after 10 min and 100% after 60 min indicating a more controlled release of ASA than from L_2 and that release of ASA from the DEX–LDH–ASA system is significantly reduced by the DEX coating[18,19].

To gain more insight into the mechanism of release of ASA from L_2 and L_3, the data were fitted to zero-order and first-kinetic equations. The results shown in Fig. 5 suggest that release is best described by a first-order equation for L_2 ($r=0.9876$) and a zero-order equation for L_3 ($r=0.9865$). Thus introducing the DEX coating prolongs the release of ASA and shifts the release pattern from first-order to zero-order. The improved controlled release from the DEX–LDH–ASA system *in vitro* led us to test its pharmacokinetics in rabbit.

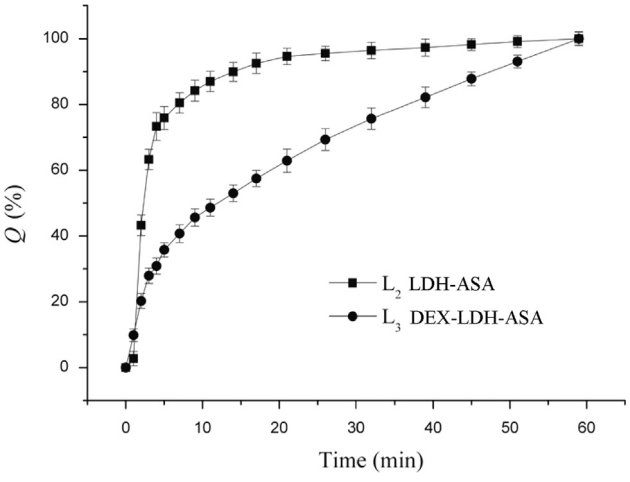

Figure 4 ASA release curves of the LDH dosing systems.

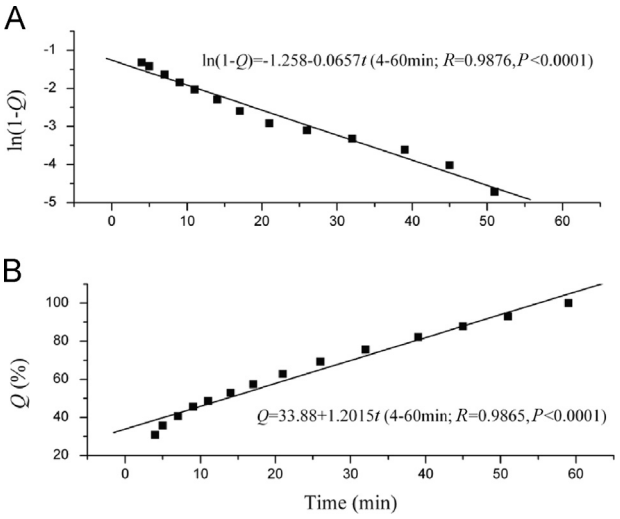

Figure 5 Fitting of ASA release from the LDH dosing systems.

3.3. *Pharmacokinetics of the DEX–LDH–ASA delivery system in rabbit*

The pharmacokinetics of SA produced by ASA hydrolysis after release from the DEX–LDH–ASA system was compared with that produced by ASA itself. Plasma concentration–time profiles and corresponding pharmacokinetic parameters are presented in Table 2 and Fig. 6. Mean plasma concentrations of ASA over 60 h show that, for ASA administration, the drug concentration rapidly reached a C_{max} of 19.63 mg/L at 1.4 h and then rapidly decreased to a trough level (0.152 mg/L) after 4 h. In contrast, after DEX–LDH–ASA administration, two absorption peaks were clearly observed. The first peak reached a C_{max} of 14.77 mg/L at 2 h after which the concentration dropped slowly to 0.423 mg/L over 10 h and then increased again to 3.455 mg/L at 16 h, finally falling to 0.199 mg/L at 60 h. The results show clearly that the DEX–LDH–ASA system provides slow release of drug *in vivo*. Moreover, it appears that oral administration of the DEX–LDH–ASA system produces a higher therapeutic trough plasma concentration, prolongs metabolic process and improves the efficacy of ASA.

There were also clear differences between the other pharmacokinetic parameters. The *in vivo* absorption half-life, clearance rate and AUC_{0-t} after administration of ASA were 0.442 h, 2.269 L/h and 21.15 mg h/L respectively, whereas after administration of the DEX–LDH–ASA system, the half-life of ASA increased by 5.08-fold, the clearance rate reduced by 51% and the oral bioavailability increased by 2.08-fold. In addition, T_{max} was delayed and C_{max} was reduced by 25%. These results show that the DEX–LDH–ASA system improves the bioavailability and decreases the elimination rate of ASA with the potential to increase its efficacy and reduce its adverse effects.

The double peak phenomenon in the pharmacokinetics of ASA administered in the DEX–LDH–ASA system is explicable in terms of its three-level supramolecular characteristics[19]. The DEX coating forms a protective network containing a large number of hydroxyl groups which not only provide an excellent antacid effect[16–18], but is also stable enough to proceed down the gastrointestinal tract[14]. In the gastrointestinal environment, rapid release of ASA on the surface together with some in the interlayer results in the first drug peak. The remaining DEX–LDH–ASA and LDH–ASA particles may be involved in enterohepatic recycling

Table 2 Principal pharmacokinetics parameters of ASA after administration of DEX–LDH–ASA and ASA to rabbits.

Parameter	ASA	DEX–LDH–ASA
$t_{1/2\alpha}$ (h)	0.442 ± 0.202	2.248 ± 0.844
AUC_{0-t} (mg · h/L)	21.15 ± 3.48	43.90 ± 5.85
CL (L/h)	2.269 ± 0.554	1.108 ± 0.231
C_{max} (mg/L)	19.63 ± 2.60	14.77 ± 1.67
T_{max} (h)	1.401 ± 0.520	2.110 ± 0.693

Data are expressed as mean ± SD, $n = 6$.

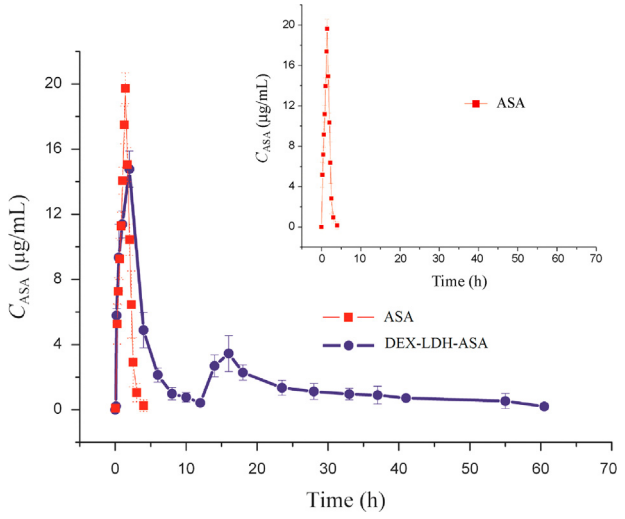

Figure 6 Plasma concentration–time curves of ASA and DEX–LDH-ASA.

and return ASA to the blood after transport *via* the hepatic portal vein leading to the second absorption peak. However, it may also originate from the delayed release of ASA from DEX–LDH–ASA and LDH–ASA nanoparticles in the blood. This would be desirable for a controlled release formulation of ASA to realize its therapeutic effects.

4. Conclusions

This work shows that a three-level supramolecular delivery system (DEX–LDH–ASA) for ASA can be successfully produced by coating an LDH–ASA complex with DEX. The crystal structure of the LDH–ASA intercalation system was largely maintained in the DEX–LDH–ASA supramolecule as demonstrated by X-ray diffraction, FT-IR spectroscopy and thermal behavior. Our results indicate that the dispersion of ASA-loaded particles and the *in vitro* and *in vivo* release of ASA from the LDH–ASA intercalation system were significantly improved. The results also show that the three-stage supramolecular assembly provides superior bioavailability of ASA and reduces its elimination rate. Overall it is clear that the DEX–LDH–ASA system has potential as an orally available controlled release drug delivery system capable of reducing the adverse effects and increasing the therapeutic efficacy of intercalated drugs.

Acknowledgment

This work was supported by the National Natural Science Foundation of China (Nos. 81260483 and 20961008).

References

1. Zhang L, Luo SD, He W, Zhang XZ, Cai HS. Pharmacokinetics of aspirin-carrying starch microspheres in rabbit as nasal administration. *Chin Hosp Pharm J* 2001;**21**:203–5.
2. Zhang ZR, You XJ, Wei ZP, He Q, Li SW. Pharmacokinetics and bioavailability of Yufeng Ningxin Jiaonang in rabbits. *Chin Pharm J* 1997;**32**:224–6.
3. Zong HX, Zhao Y, Li J. Studies on preparation, release and pharmacokinetics of aspirin sustained release tablets. *Chin Pharm J* 2000;**35**:110–3.
4. Wang YL, Wang GH, Li XM. Study on aspirin enteric-coated tablets release in beagles. *Northwest Pharm* 2010;**25**:42–4.
5. Gou GJ, Ma PH, Chu MX. Preparation and basic properties of layered double hydroxides intercalated by chloride anion. *Acta Chim Sin* 2004;**62**:2150–60.
6. Del Arco M, Cebadera E, Gutiérrez S, Martín C, Montero MJ, Rives V, et al. Mg Al layered double hydroxides with intercalated indomethacin: synthesis, characterization, and pharmacological study. *J Pharm Sci* 2004;**93**:1649–58.
7. Wang ZL, Wang EB, Tian SY, Xiao DR, Gao L, Wang L, et al. Intercalation of PM-19 into and *in vitro* release of anti-tumor drug from layered double hydroxide. *Chem Res Chin Univ* 2005;**21**:492–5.
8. Ladewig K, Xu ZP, Lu GQ. Layered double hydroxide nanoparticles in gene and drug deliver. *Expert Opin Drug Deliv* 2009;**9**:907–22.
9. Ambrogi V, Fardella G, Grandolini G, Perioli L. Intercalation compounds of hydrotalcite-like anionic clays with antiinflammatory agents—I. Intercalation and *in vitro* release of ibuprofen. *Int J Pharm* 2001;**220**:23–32.
10. Choi SJ, Oh JM, Choy JH. Biocompatible nanoparticles intercalated with anticancer drug for target delivery: pharmacokinetic and biodistribution study. *J Nano Sci Nano Technol* 2010;**10**:2913–6.
11. Oh JM, Park CB, Choy JH. Intracellular drug delivery of layered double hydroxide nanoparticle. *J Nano Sci Nano Technol* 2011;**11**:1632–5.
12. Al Ali SHH, Al-Qubaisi M, Hussein MZ, Ismail M, Zainal Z, Hakim MN. Controlled release and angiotensin-converting enzyme inhibition properties of an antihypertensive drug based on a perindopril erbumine-layered double hydroxide nanocomposite. *Int J Nano* 2012;**7**:2129–41.
13. Gou GJ, Xu HP, Liu JP. Loading and *in vitro* release of acetylsalicylic acid *via* layered double hydroxides. *Acta Chim Sin* 2009;**67**:65–82.
14. Wang ZI, Wang EB, Gao L, Xu L. Synthesis and properties of Mg_2Al layered double hydroxides containing 5-fluorouracil. *J Solid State Chem* 2005;**178**:736–41.

15. Gou GJ, Liu YH, Sun Y, Huang J, Xue B. Ion exchange reaction kinetics of magnetic layered double hydroxides with 5-fluorouracil. *Chem J Chin Univ* 2012;**33**:119–27.
16. Brich Z, Ravel S, Kissel T, Fritsch J, Schoffmann A. Preparation and characterization of a water soluble dextran immunoconjugate of doxorubicin and the monoclonal antibody. *J Control Release* 1992;**19**: 245–57.
17. Tassa C, Shaw SY, Weissleder R. Dextran-coated iron oxide nanoparticles: a versatile platform for targeted molecular imaging, molecular diagnostics and therapy. *Acc Chem Res* 2011;**44**:842–52.
18. Jiao L, Gou GJ, Yang JH, Yang XP, Zhu YS, Yan QS, et al. Effects of dextran and hpmc on sustained-release property of ldh-acetosalicylic acid system. *Chin Pharm J* 2011;**46**:357–63.
19. Gou GJ, Liu YH, Sun Y, Huang J, Xue B, Dong LE. The supramolecular assembly and magnetic targeted slow-release effect of "dextran – magnetic layered double hydroxide – fluorouracil" drug delivery system. *Acta Pharm Sin* 2011;**46**:1390–8.
20. Huang J, Gou GJ, Xue B, Yan QS, Sun Y, Dong LE. Preparation and characterization of dextran–magnetic layered double hydroxide-fluorouracil targeted liposomes. *Int J Pharm.* 2013;**450**:323–30.